

## Simulation Models for Stem Cells Differentiation

M. Pisu,<sup>a</sup> A. Concas,<sup>b</sup> and G. Cao<sup>c,\*</sup>

<sup>a</sup>Center for Advanced Studies, Research and Development in Sardinia (CRS4)

<sup>b</sup>Center for Advanced Studies, Research and Development in Sardinia (CRS4)

<sup>c</sup>University of Cagliari and Center for Advanced Studies, Research and Development in Sardinia (CRS4)

Original scientific paper

Received: April 3, 2012

Accepted: July 26, 2012

A novel mathematical model to simulate stem cells differentiation into specialized cells of connective or non-connective tissues is discussed. The model is based upon material balances for extra cellular matrix compounds, growth factors and nutrients coupled with a mass-structured population balance describing cell growth, proliferation and differentiation. The model is written in a general form and it may be used to simulate a generic cell differentiation pathway occurring *in vivo* or during *in vitro* cultivation when specific growth factors are used. Several examples are discussed where literature experimental data are successfully compared with model results, thus demonstrating the validity of the proposed model as well as its predictive capability.

*Key words:*

Stem cells differentiation, modeling, population, balance

### Introduction

Stem cells are currently receiving a great attention since they represent a potential source of cells for transplantation. In fact these cells have the ability to self-renew and differentiate into functional cells of various tissues.<sup>1,2</sup> Proliferative capacity of many adult tissue-specific cells is very limited, so that their expansion *in vitro* results to be difficult, even during long-term cultivation which in addition reduces their functional quality. Thus, attention is currently devoted to the use of stem cells or progenitor ones instead of tissue-specific cells.<sup>3</sup> Adult stem cells may be obtained from tissues (liver, intestine, retina, skin, muscle, mammary glands and others) of individual patients so that reimplantation of *in vitro* cultivated cells/tissues would avoid problems of rejection. Despite this very attractive opportunity, the use of adult stem cells is limited by the ability to identify these rare cells from the heterogeneous tissue population and to expand them *in vitro*.<sup>2</sup> Mesenchymal stem cells (MSCs), also known as marrow stromal cells, which are progenitors of all tissue cells, can be on the other hand isolated using standard techniques, expanded in culture, and stimulated to differentiate into the desired tissues.<sup>4,5</sup> MSCs may differentiate into specialized cells to form bone, cartilage, tendon, dermal, adipose and muscle tissues. In addition, MSCs may differentiate into hepatic, renal, cardiac and neural stem cells.<sup>6</sup> These properties open up therapeutic

opportunities for the treatment of lesions in mesenchymal tissues so that protocols have been devised for the treatment of defects in articular cartilage, bone, tendon, meniscus and for bone marrow stromal recovery and osteogenesis imperfecta.<sup>5</sup> When forming connective tissues, cells secrete macromolecules (collagen and proteoglycans mainly represented by glycosaminoglycan, GAG) which constitute the extra-cellular matrix (ECM). The latter provides an organized environment wherein migratory cells can move and interact with one another and stationary cells are anchored.<sup>3</sup> Recent studies suggested that the use of three-dimensional scaffold may improve, quantitatively, the differentiation of stem cells.<sup>7,8</sup> These investigations are focused on the identification of the more suitable cultivation scaffolds and the optimization of the mechanical and physical properties of such materials. A very important role on cell differentiation is played by growth factors (GFs), which are proteins that bind to receptors on the cell surface, with the primary result of activating cellular proliferation and/or differentiation. Many growth factors are quite versatile, stimulating cellular division in several different cell types, while others are specific to a particular cell-type. Among the various growth factors, bone morphogenetic protein (*BMP*) which belongs to the transforming growth factor- $\beta$  (*TGF- $\beta$* ) superfamily, plays an important role in the regulation of the differentiation pathway of MSCs.<sup>9</sup> In particular, these growth factors may induce the differentiation of MSCs into connective cells such as osteoblasts, chondrocytes and adipocytes.<sup>9</sup> Several papers are focused on experimental studies

\*Correspondence: Dipartimento di Ingegneria Meccanica, Chimica e Materiali, Università di Cagliari, Piazza d'Armi, I-09123 Cagliari, Italy

concerning the mesenchymal stem cell differentiation into chondrocytes stimulated by *TGF- $\beta$*  superfamily.<sup>5,10–17</sup> Further studies are required since the effect of this type of growth factors are in some cases contradictory and mechanisms concerning cell proliferation/differentiation and the interaction with growth factors need to be elucidated.

An important contribution along these lines may be provided by predictive models which should facilitate the experiments, thus helping to find the optimal operating conditions and at the same time contributing to the understanding of biological mechanisms and stem cell behavior. For this reason several contributions on the modeling of these systems are available starting with the stochastic model of stem cell proliferation proposed by Till et al.<sup>18</sup> More recently, a remarkable attempt to simulate cell differentiation for ex-vivo hematopoiesis in the presence of *TGF- $\beta$ 1* is done by.<sup>19</sup> These authors developed a mathematical model based on population balance (PB) which describes the hematopoiesis starting from a colony of hematopoietic stem cell. The model uses a tank and tubular reactor metaphor to describe the (pseudo)-stochastic and deterministic elements of hematopoiesis. Bailon-Plaza and van der Meulen<sup>20</sup> proposed a two-dimensional mathematical model for simulating the effect of growth factor on fracture healing. The model describes the differentiation of mesenchymal stem cells into chondrocytes and osteoblasts during a fracture healing by accounting for material balance of the involved cells (mesenchyms, chondrocytes and osteoblasts) together with a material balance on ECMs and growth factors. In addition, Hentschel et al.<sup>21</sup> developed a mathematical model which describes the dynamic mechanisms for skeletal pattern formation in the vertebrate limb when growth factors (fibroblast growth factor, *FGF*, and *TGF- $\beta$ s*) are present. Beside the works considered above, other authors have addressed the simulation of cell differentiation. For the sake of brevity, a list of the most interesting models available in the literature on this subject is summarized in table 1. The main limitation of these models is represented by the absence of the description of the cell size distribution and its influence on cellular metabolism and differentiation.

In this paper, we propose a novel mathematical model to simulate stem cells differentiation into specialized cells. The model, along the lines of our previous contributions<sup>27–31</sup> is based upon material balances for extra cellular matrix compounds, growth factors and nutrients as well as mass-structured population balance to simulate cell growth, differentiation and proliferation in vivo or during in vitro cultivation. The proposed model is written in a general form and may be used to simulate a generic

Table 1 – Models concerning the simulation of cell differentiation processes

Model	Reference
Stochastic model of stem cell proliferation for spleen colony-forming cells	[18]
Model of differentiation processes in the thymus	[22]
Stochastic model of brain cell differentiation	[23]
Pseudo-stochastic and deterministic model for ex-vivo hematopoiesis	[19]
Stochastic model of proliferation and differentiation of O2-A progenitor cells	[24]
Deterministic two-dimensional model on fracture healing	[20]
Dynamic mechanisms for skeletal pattern formation in the vertebrate limb in the presence of growth factors	[21]
Dynamic model for cellular differentiation and co-expression properties of switch networks	[25]
Mathematical model for the interaction of transcription factors	[26]

cell differentiation pathway occurring during in vitro cultivation of connective and non-connective tissues. Literature experimental data concerning the differentiation of mesenchymal stem cells into chondrocytes in terms of total DNA and GAG content are successfully compared with model results, thus demonstrating the validity of the proposed model as well as its predictive capability. In addition, literature experimental data concerning the differentiation of murine central nervous stem cells into astrocytes are also successfully compared with model results, thus further demonstrating the validity of the proposed model as well as its predictive capability.

### Mathematical modeling

The proposed mathematical model for stem cell differentiation into connective or non-connective tissues is based on the pathway schematically shown in Fig. 1. Stem cells may differentiate into specialized cells of type 1 under the influence of specific growth factors  $GF_1$ . Stem cells may also differentiate into specialized cells of type 2 by means of a different class of growth factors  $GF_2$ . These cells may be also obtained by the differentiation of specialized cells of type 1 under the influence of the specific growth factor  $GF_2$ . All the cells involved in the pathway shown in Fig. 1 undergo mitosis and may synthesize two extra cellular matrix compounds, i.e. ECM1 and ECM2. This scheme may involve more cell types and different pathways of cell specialization starting from a stem

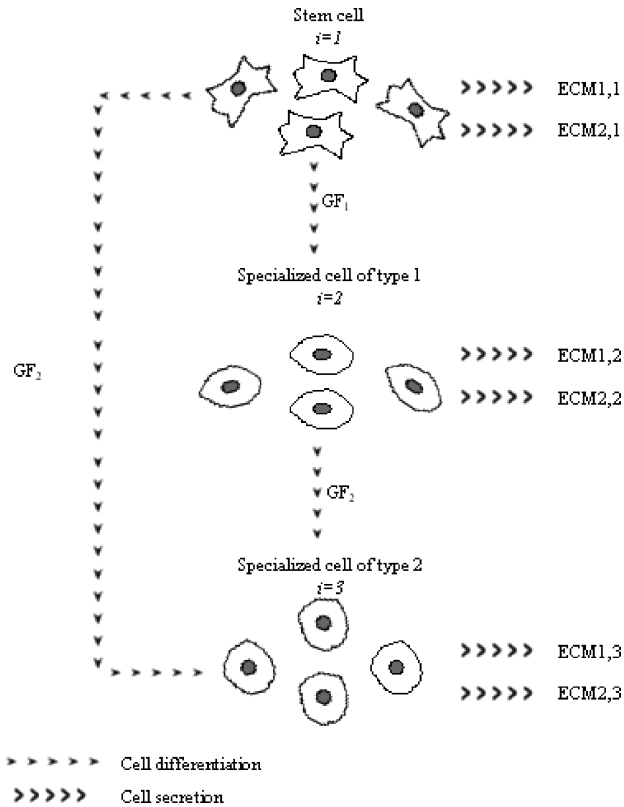


Fig. 1 – Schematic representation of the cell differentiation pathways. Stem cells may differentiate into specialized cells of type 1 under the influence of specific growth factors  $GF_1$ . Stem cells may also differentiate into specialized cells of type 2 by means of a different class of growth factors  $GF_2$ . These cells may be also obtained by the differentiation of specialized cells of type 1 under the influence of the same growth factor  $GF_2$ .

cell population ( $i=1$ ). It is apparent that the pathway shown in Fig. 1 can be simplified when the differentiation into non-connective tissues is taking into account. In the latter case the presence of ECM is non accounted for.

As it may be seen, the mathematical model is able to simulate cell growth, proliferation and differentiation into intermediate or specialized cells during cell cultivation in the presence of culture medium and specific growth factors. The model accounts for the ECM compounds secreted by cells and is aimed to quantitatively describe the effect of growth factors during cell differentiation. The model is written in a general form and may be used for simulating the differentiation of stem cells into intermediate and specialized cells of various type. Thus, by properly modifying the network scheme, growth kinetics and differentiation rate expressions, this model may be used to simulate and describe different pathologies involving cell growth and differentiation (i.e. tumors development, infections, arthritis, etc.) or to guide the investigation on *in vitro/in vivo* cell cultivation, growth and differentiation in tissue engineering.

Specifically, the proposed model is based on the following mass structured population balance for the generic cell of  $i$ -th type:

$$\frac{\partial \psi_i(m_i, t)}{\partial t} + \frac{\partial [v_i \psi_i(m_i, t)]}{\partial m_i} = \int_m^\infty \psi_i(m'_i, t) \Gamma_i^F(m'_i, C_{O_2}) p(m_i, m'_i) dm'_i - \psi_i(m_i, t) \Gamma_i^F(m_i, C_{O_2}) + \psi_k(m_k, t) \Gamma_{kj}^T(m_k, C_{GF,j}) - \psi_i(m_i, t) \Gamma_{ij}^T(m_i, C_{GF,j}) \quad \text{for } i = 1, \dots, N_C \text{ and } k \neq i$$

along with

$$\psi_i(m, t) = \psi_i^0(m, 0) \quad \text{for } t = 0 \text{ and } m > 0 \quad (2)$$

$$\psi_i(m, t) = 0 \quad \text{for } t > 0 \text{ and } m = 0 \quad (3)$$

where symbol's significance is reported in the notation. In equation (1) the first two terms of the right-hand-side represent the birth (i.e. a mother cell may be divided in two daughter cells) and the death of the cell of  $i$ -th type due to mitosis. The third term of the right-hand-side of equation (1) accounts for the gain of the cell of  $i$ -th type due to differentiation from cells of  $k$ -th type (with  $k \neq i$ ) as stimulated by the  $j$ -th growth factor. Finally, the fourth term is represented by the loss of the cell of  $i$ -th type due to differentiation. It is worth mentioning that the cellular death by apoptosis is neglected since it may be relevant only in the case of apoptotic/necrotic tissues.

By considering the approach described in detail in previous works [27–31] cell mitotic fraction,  $\Gamma_i^F$ , and the cell mass growth rate,  $v_i$ , appearing in equation (1) are expressed as follows:

$$\Gamma_i^F(m_i, C_{O_2}) = \frac{v_i(m_i, C_{O_2}) f(m_i)}{1 - \int_0^m f(m'_i) dm'_i} \quad (4)$$

$$v_i(m_i, C_{O_2}) = \left( \frac{3}{d_{c,i}} \right)^{2/3} (4\pi)^{1/3} m_i^{2/3} \frac{\mu'_i C_{O_2}}{C_m + C_{O_2}} - \mu_{c,i} m_i \quad (5)$$

where

$$f(m) = \frac{1}{\sqrt{2\pi\sigma_i^2}} \exp \left( -\frac{(m - \mu_{0,i})^2}{2\sigma_i^2} \right) \quad (6)$$

$$p(m, m') = \frac{1}{\beta(q_i, q_i)} \frac{1}{m'} \left( \frac{m}{m'} \right)^{q_i-1} \left( 1 - \frac{m}{m'} \right)^{q_i-1} \quad (7)$$

On the other hand, by taking into account its dependence upon the specific growth factor con-

centration up to a maximum constant saturation value<sup>20</sup> the differentiation rate  $\Gamma_{ij}^T$  is expressed as follows:

$$\Gamma_{ij}^T = \frac{a_{ij}C_{GF_j}}{b_{ij} + C_{GF_j}} \quad (8)$$

By assuming negligible mass transfer, population balance (1), along with initial (2) and boundary conditions (3) and equations (4)-(8) are coupled with the following material balances for ECM1 and ECM2:

$$\frac{dC_{ECM1,i}}{\partial t} = k_{ECM1,i} \left( \int_0^\infty m_i \psi_i(m_i, t) dm_i \right) \left( 1 - \frac{C_{ECM1,i}}{C_{ECM1,i}^L} \right) C_{O_2}$$

for  $i = 1, \dots, N_C$  (9)

$$\frac{dC_{ECM2,i}}{\partial t} = k_{ECM2,i} \left( \int_0^\infty m_i \psi_i(m_i, t) dm_i \right) \left( 1 - \frac{C_{ECM2,i}}{C_{ECM2,i}^L} \right) C_{O_2}$$

for  $i = 1, \dots, N_C$  (10)

where symbol's significance is reported in the notation.

Extracellular matrix, quantitatively described by equations (9)-(10), is secreted by the cell of the  $i$ -th type, whose differentiation is promoted by growth factor  $j$ . It should be noted that the reactive terms of equations (9)-(10), which describe ECM1 and ECM2 synthesis, respectively, are written in form of a *product-inhibited kinetics*, as discussed in previous works [27–31] and account for the total cellular mass per unit volume (i.e.  $\left( \int_0^\infty m_i \psi_i(m_i, t) dm_i \right)$ ). It should be also noted that in equations (9)-(10) the degradation of ECM compounds is not considered. The growth factor concentration as a function of time is simulated by the present model either in the case of *in vitro* (eq. 11a) or in the case of *in vivo* cultivation (eq. 11b):

$$\frac{dC_{GF_1}}{\partial t} = - \sum_i \chi_{ij} \left( \int_0^\infty m_i \psi_i(m_i, t) dm_i \right) \frac{a_{ij}C_{GF_j}}{b_{ij} + C_{GF_j}}$$

for  $j = 1, \dots, N_{GF}$  (*in vitro*) (11a)

$$\frac{dC_{GF_1}}{\partial t} = - \sum_i \chi_{ij} \left( \int_0^\infty m_i \psi_i(m_i, t) dm_i \right) \frac{a_{ij}C_{GF_j}}{b_{ij} + C_{GF_j}} + k_{GF_j}^B \sum_k \left( \int_0^\infty m_k \psi_k(m_k, t) dm_k \right)$$

for  $j = 1, \dots, N_{GF}$  (*in vivo*) (11b)

where symbols' significance is reported in the notation.

Equation (11), which describes the growth factor consumption, accounts for a yield  $\chi_{ij}$  which relates, as discussed in what follows, the differentiation rate of the generic  $i$ -th cell to the consumption of the  $j$ -th growth factor. If cell differentiation occurs *in vivo* (as in the case of the fracture healing described by Bailon-Plaza and van der Meulen<sup>20</sup> an additional term should be introduced to account for the local growth factor production which is assumed to be proportional to the mass of cell of  $k$ -th type, as it may be seen in equation (11b).

The following initial conditions for equations (9)-(11), for which symbols' significance is reported in the notation, hold:

$$C_{ECM1,i} = C_{ECM1,i}^0; \quad C_{ECM2,i} = C_{ECM2,i}^0 \quad \text{and}$$

$$C_{GF_j} = C_{GF_j}^0 \quad \text{at } t = 0 \quad (12)$$

When considering the case of non-connective tissues, the model described above consists of equations (1)-(8) and (11) while in equation (12) only the initial condition related to growth factors is taken into account.

The system of ordinary differential equations (9)-(11) along with initial conditions (12) requires the knowledge of the cell distribution function,  $\psi_i$  of  $i$ -th type of cells, which is obtained from the solution of the population balance expressed by equation (1). It represents a partial differential equation in the variables  $t$  and  $m$ , which is solved by discretizing the derivative whose independent variable is the cell mass  $m$ . After the choice of the upper limit, the mass domain is divided using a constant step size mesh, and only the partial derivative with respect to  $m$  is discretized by backward finite difference. Thus, the partial integro-differential equation (1) is transformed into a system of ordinary differential equations. The latter one, coupled with equations (9)-(11) along with initial conditions (12), represents a larger system of ordinary differential equations which is solved as an initial value problem with the Gear method by taking advantage of standard numerical libraries. 101 grid points (including the first one which corresponds to  $m=0$ ) in the mass domain are typically used for numerically solving the PB model, since finer grids did not provide significant improvements in accuracy.

## Results and discussion

Let us consider as a first example to demonstrate the validity of the proposed model approach, the case of stem cell differentiation in specialized

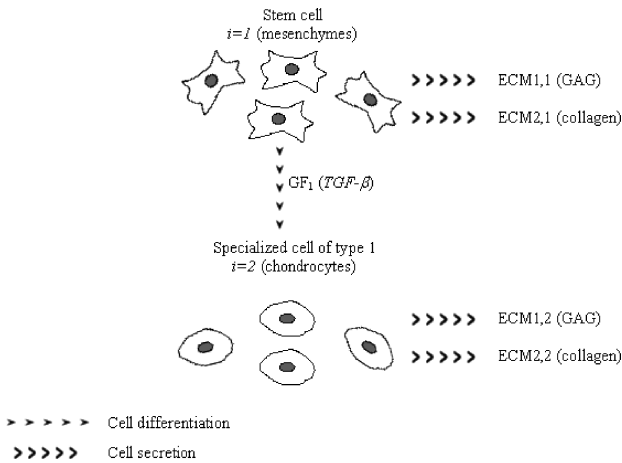


Fig. 2 – Schematic pathway for mesenchymal cells differentiation into chondrocytes stimulated by  $TGF-\beta$

cells of connective tissues. The case study refers to the differentiation of mesenchymal stem cells (MSCs) into chondrocytes cells (CCs) stimulated by a specific growth factor of  $TGF-\beta$  family. Mesenchymes and chondrocytes may secrete GAG and collagen as extracellular matrix components. For this application the general differentiation pathway reported in Fig. 1 may be simplified as shown in Fig. 2.

To test the capabilities of the proposed model we take advantage of experimental data reported by Barry et al.<sup>5</sup> who investigated the *in vitro* chondrogenic differentiation of human mesenchymal stem cells from bone marrow by means of different growth factors (i.e.,  $TGF-\beta1$ ,  $TGF-\beta2$  and  $TGF-\beta3$ ). They isolated and centrifuged MSCs to obtain one culture pellet and cultivated for 21 days under culture medium in presence of  $TGF-\beta1$ , or  $TGF-\beta2$  or  $TGF-\beta3$ . Experimental data were reported in terms of DNA and GAG content for each experiment performed. Firstly, model results are directly compared with experimental data obtained when growth factor  $TGF-\beta1$  was used. It should be noted that the cell content is here expressed as  $\mu g$  of DNA where the characteristic weight of 7.7 pg of DNA per cell has been assumed (Wilson et al., 2002). Model parameters used in simulation run, whose values are reported in table 2, were taken from the literature related to either the original work from which the experimental data have been generated or to specific sources where the corresponding values are available. Fig. 3a and 3b show a good agreement between model results and experimental data in terms of DNA and GAG content as a function of cultivation time. It is worth noting that the unknown model parameters (i.e., kinetic constants for GAG synthesis,  $k_{ECM1,i}$  appearing in equation (9) and parameters  $a_{II}$ ,  $b_{II}$  and  $\chi_{II}$  of equation (3)) are estimated by means of a nonlinear least-square pro-

Table 2 – Model parameters used in the simulation of mesenchymal stem cells differentiation into chondrocyte cells stimulated by  $TGF-\beta1$  ( $i=1$  for MSCs,  $i=2$  for CCs;  $j=1$  for  $TGF-\beta1$ ). Experimental data from Barry et al.<sup>5</sup> The regression analysis provides an average percentage error of 22.0.

Parameter	Value	Unit	Reference
$\rho_i^0$ ( $i=1$ )	$2.0 \cdot 10^5$	cells/pellet	[5]
$C_{GF_j}^0$ ( $j=1$ )	$10 \cdot 10^{-3}$	ng/mm <sup>3</sup>	[5]
$C_{ECM1,i}^0$ ( $i=1$ )	3	dw%	[5]
$C_{ECM1,i}^0$ ( $i=2$ )	0	dw%	[5]
$C_{ECM2,i}^0$ ( $i=1,2$ )	0	dw%	[5]
$C_{ECM1,i}^L$ ( $i=1,2$ )	11.7	dw%	[32]
$C_{ECM2,i}^L$ ( $i=1,2$ )	50.4	dw%	[32]
$dc_i$ ( $i=1,2$ )	$1.14 \cdot 10^6$	ng/mm <sup>3</sup>	[33]
$d_{ECM1,i}$ ( $i=1,2$ )	$1.85 \cdot 10^6$	ng/mm <sup>3</sup>	[34]
$d_{ECM2,i}$ ( $i=1,2$ )	$1.44 \cdot 10^6$	ng/mm <sup>3</sup>	[34]
$d_w$	$1.0 \cdot 10^6$	ng/mm <sup>3</sup>	[35]
$C_{O_2}$	$0.124 \cdot 10^{-6}$	mmol/mm <sup>3</sup>	[36]
$C_m$	$0.006 \cdot 10^{-6}$	mmol/mm <sup>3</sup>	[36]
$\mu_{0,i}$ ( $i=1,2$ )	0.4	ng	[37]
$\sigma_i$ ( $i=1,2$ )	0.125	ng	[38]
$q_i$ ( $i=1,2$ )	40	–	[38]
$\mu_{C,i}$ ( $i=1,2$ )	$1.0 \cdot 10^{-3}$	1/h	[39]
$\mu_i'$ ( $i=1,2$ )	2.646	ng/(mm <sup>2</sup> h)	[29]
$k_{ECM2,i}$ ( $i=1,2$ )	$0.015 \cdot 10^3$	dw% mm <sup>6</sup> /(ng mmol h)	[29]
$k_{ECM1,i}$ ( $i=1,2$ )	$1.23 \cdot 10^3$	dw% mm <sup>6</sup> /(ng mmol h)	[30]
$a_{ij}$ ( $i=1; j=1$ )	0.76	1/h	[30]
$b_{ij}$ ( $i=1; j=1$ )	$1.01 \cdot 10^{-3}$	ng/mm <sup>3</sup>	[30]
$\chi_{ij}$ ( $i=1; j=1$ )	$5.80 \cdot 10^{-3}$	ng of GF/ng of cells	[30]

cedure against the experimental data. The regression analysis gives rise to an average percentage error of 22.0. Analogously, model results were compared with experimental data obtained when cultivation was carried out by using growth factor  $TGF-\beta2$ . Model parameters used in this simulation run are reported in table 3.

Also in this case, as shown in Fig. 4a and 4b, the agreement between model results and experimental data is satisfactory and the regression analysis provides an average percentage error of 10.2.

It should be noted that, since the experimental data used so far are given in terms of DNA mass, the population balance adopted in our model would have been based on DNA mass as internal variable. However, cell mass-structured population balances

Table 3 – Model parameters used in the simulation of mesenchymal stem cells differentiation into chondrocyte cells stimulated by  $TGF-\beta 2$  or  $TGF-\beta 3$  ( $i=1$  for MSCs,  $i=2$  for CCs;  $j=1$  for  $TGF-\beta 1$  or  $TGF-\beta 3$ ). Experimental data from Barry et al.<sup>5</sup> The regression analysis provides an average percentage error of 10.2.

Parameter	Value	Unit	Reference
$\rho_i^0$ ( $i=1$ )	$2.0 \cdot 10^5$	cells/pellet	[5]
$C_{GF_j}^0$ ( $j=1$ )	$10 \cdot 10^{-3}$	ng/mm <sup>3</sup>	[5]
$C_{ECM1,i}^0$ ( $i=1$ )	3	dw%	[5]
$C_{ECM1,i}^0$ ( $i=2$ )	0	dw%	[5]
$C_{ECM2,i}^0$ ( $i=1,2$ )	0	dw%	[5]
$C_{ECM1,i}^L$ ( $i=1,2$ )	11.7	dw%	[32]
$C_{ECM2,i}^L$ ( $i=1,2$ )	50.4	dw%	[32]
$dc_i$ ( $i=1,2$ )	$1.14 \cdot 10^6$	ng/mm <sup>3</sup>	[33]
$d_{ECM1,i}$ ( $i=1,2$ )	$1.85 \cdot 10^6$	ng/mm <sup>3</sup>	[34]
$d_{ECM2,i}$ ( $i=1,2$ )	$1.44 \cdot 10^6$	ng/mm <sup>3</sup>	[34]
$d_w$	$1.0 \cdot 10^6$	ng/mm <sup>3</sup>	[35]
$C_{O_2}$	$0.124 \cdot 10^{-6}$	mmol/mm <sup>3</sup>	[36]
$C_m$	$0.006 \cdot 10^{-6}$	mmol/mm <sup>3</sup>	[36]
$\mu_{0,i}$ ( $i=1,2$ )	0.4	ng	[37]
$\sigma_i$ ( $i=1,2$ )	0.125	ng	[38]
$q_i$ ( $i=1,2$ )	40	–	[38]
$\mu_{C,i}$ ( $i=1,2$ )	$1.0 \cdot 10^{-3}$	1/h	[39]
$\mu_i'$ ( $i=1,2$ )	2.646	ng/(mm <sup>2</sup> h)	[29]
$k_{ECM2,i}$ ( $i=1,2$ )	$0.015 \cdot 10^3$	dw% mm <sup>6</sup> /(ng mmol h)	[29]
$k_{ECM1,i}$ ( $i=1,2$ )	$4.99 \cdot 10^3$	dw% mm <sup>6</sup> /(ng mmol h)	[30]
$a_{ij}$ ( $i=1; j=1$ )	0.73	1/h	[30]
$b_{ij}$ ( $i=1; j=1$ )	$0.01 \cdot 10^{-3}$	ng/mm <sup>3</sup>	[30]
$\chi_{ij}$ ( $i=1; j=1$ )	$0.10 \cdot 10^{-3}$	ng of GF/ng of cells	[30]

of the type adopted in this work seem more appropriate when describing metabolic/mitotic/differentiation processes which are directly related to cell size and thus to the corresponding mass.

To test the predictive model capability, the experimental data performed with  $TGF-\beta 3$  are then simulated. This growth factor has a comparable effect with respect to  $TGF-\beta 2$  on mesenchymal differentiation into chondrocytes.<sup>5</sup> By using the same parameters of table 3, i.e. without any fitting procedure, model predictions and experimental data by Barry et al.<sup>5</sup> were compared in terms of DNA and GAG content as a function of cultivation time. The good agreement between model results and experimental data shown in Figs 5a and 5b demonstrates the predictive capability of the model.

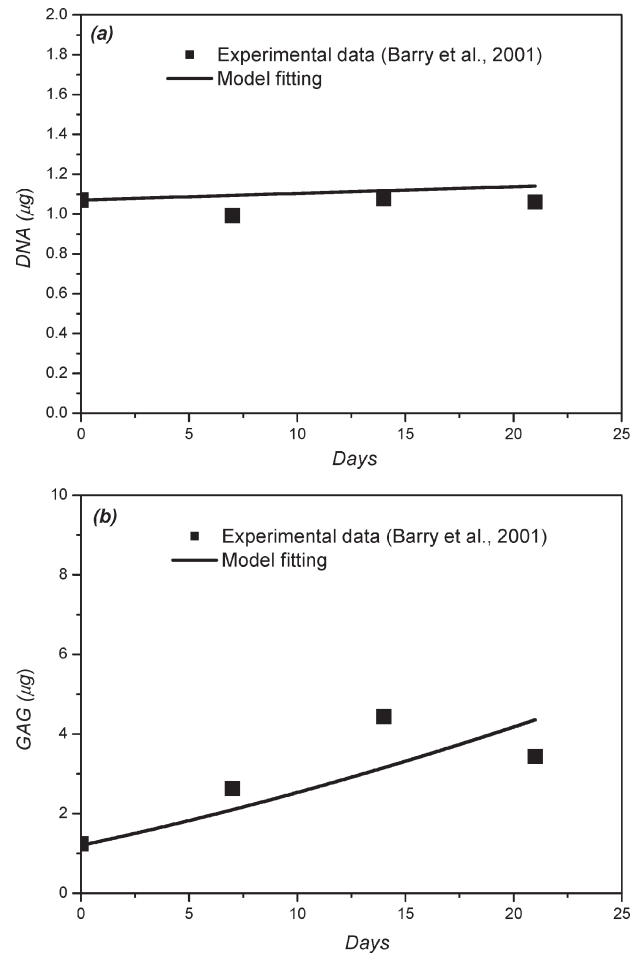


Fig. 3 – Comparison between model results and experimental data in terms of DNA (a) and GAG content (b) as a function of culture time for experiments carried out with  $TGF-\beta 1$  (Experimental data from Barry et al.<sup>5</sup>).

A further example which clearly shows the model capabilities is represented by the simulation of the effect of the growth factor concentration in the culture medium when considering experimental data by Bai et al.<sup>12</sup> These data refer to *in vitro* differentiation of human mesenchymal stem cell from bone marrow into chondrocyte cells. In this case MSCs were isolated, centrifuged to obtain a culture pellet and cultivated for 21 days under a culture medium in presence of  $TGF-\beta 1$  and/or  $CDMP-1$  (cartilage-derived morphogenic protein-1). In particular, experimental data concerning GAG content within the pellet after 21 days of cultivation as a function of different concentration of growth factor  $CDMP-1$  (from 50 to 500 ng/ml) with a constant quantity of  $TGF-\beta 1$  (10 ng/ml) has been simulated.<sup>30</sup> Also in this case model parameters (reported in table 4) used in the simulation are taken from the literature related to either the original work from which the experimental data have been generated or to specific sources where the corresponding values are available. It should be noted

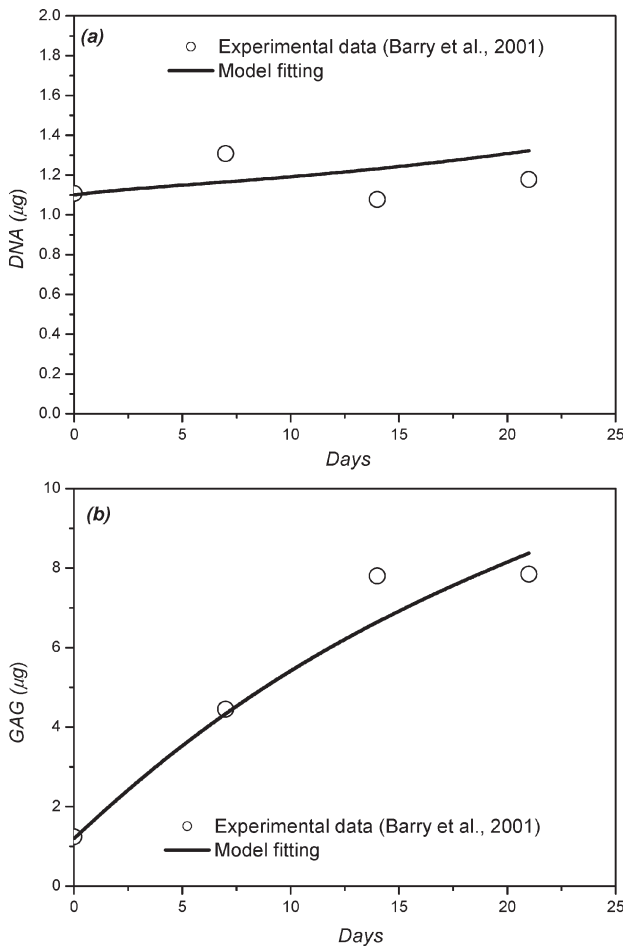


Fig. 4 – Comparison between model results and experimental data in terms of DNA (a) and GAG content (b) as a function of culture time for experiments carried out with TGF- $\beta$ 2 (Experimental data from Barry et al.<sup>5</sup>).

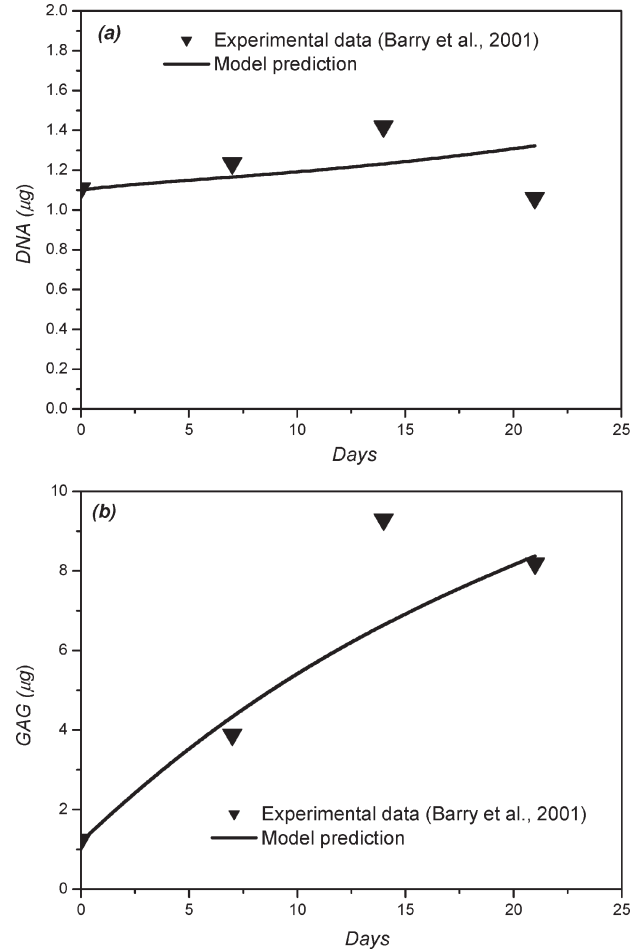


Fig. 5 – Comparison between model predictions and experimental data in terms of DNA (a) and GAG content (b) as a function of culture time for experiments carried out with TGF- $\beta$ 3 (Experimental data from Barry et al.<sup>5</sup>).

that the unknown model parameters (i.e., kinetic constants for GAG synthesis,  $k_{ECM1,2}$  and parameters  $a_{II}$ ,  $b_{II}$  and  $\chi_{II}$ ) were tuned to fit the GAG contents after 21 days of cultivation when a concentration of CDMP-1 equal to 100 ng/ml was used. Thus, by employing these parameters, the remaining experimental data were predicted by the model as shown in Fig. 6. The agreement between model results and experimental data is satisfactory and confirms the predictive capability of the proposed model.

Finally, the reliability of the mathematical modeling approach based on PB is tested by considering the differentiation of central nervous system stem cells into astrocytes cells stimulated by a specific growth factor.<sup>31</sup> The differentiation pathway reported in Fig. 1 may be simplified as shown in Fig. 7.

The mathematical model for simulating stem cell differentiation into specialized cells of non-connective tissues is also simplified accordingly, as discussed in the Modeling section. In this

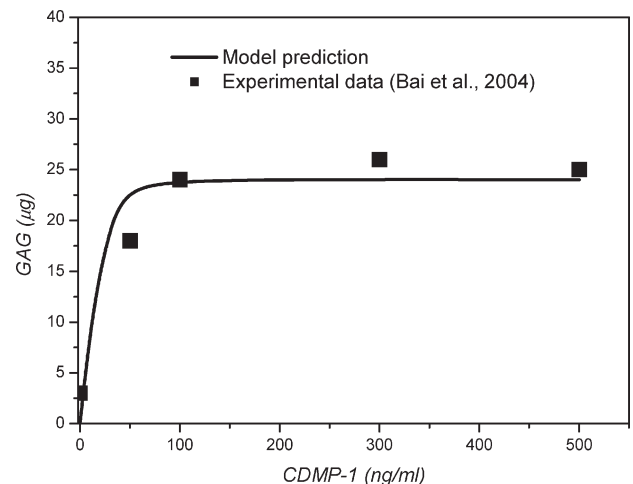


Fig. 6 – Comparison between model predictions and experimental data in terms of GAG content after 21 days of cultivation as a function of different concentration of CDMP-1 (Experimental data from Bai et al.<sup>12</sup>).

example, mathematical model results are compared with experimental data reported by Satoh et al.<sup>40</sup>

Table 4 – Model parameters used in the simulation of mesenchymal stem cells differentiation into chondrocyte cells stimulated by CDMP-1 ( $i=1$  for MSCs,  $i=2$  for CCs;  $j=1$  for CDMP-1). Experimental data from Bai et al.<sup>12</sup> (0, 50, 100, 300, 500 ng/ml of CDMP-1 with addition of 10 ng/ml TGF- $\beta$ 1).

Parameter	Value	Unit	Reference
$\rho_i^0$ ( $i=1$ )	$2.5 \cdot 10^5$	cells/pellet	[5]
$C_{ECM1,i}^0$ ( $i=1,2$ )	0	dw%	[5]
$C_{ECM2,i}^0$ ( $i=1,2$ )	0	dw%	[5]
$C_{ECM1,i}^L$ ( $i=1,2$ )	11.7	dw%	[32]
$C_{ECM2,i}^L$ ( $i=1,2$ )	50.4	dw%	[32]
$dc_i$ ( $i=1,2$ )	$1.14 \cdot 10^6$	ng/mm <sup>3</sup>	[33]
$d_{ECM1,i}$ ( $i=1,2$ )	$1.85 \cdot 10^6$	ng/mm <sup>3</sup>	[34]
$d_{ECM2,i}$ ( $i=1,2$ )	$1.44 \cdot 10^6$	ng/mm <sup>3</sup>	[34]
$d_w$	$1.0 \cdot 10^6$	ng/mm <sup>3</sup>	[35]
$C_{O_2}$	$0.124 \cdot 10^{-6}$	mmol/mm <sup>3</sup>	[36]
$C_m$	$0.006 \cdot 10^{-6}$	mmol/mm <sup>3</sup>	[36]
$\mu_{0,i}$ ( $i=1,2$ )	0.4	ng	[37]
$\sigma_i$ ( $i=1,2$ )	0.125	ng	[38]
$q_i$ ( $i=1,2$ )	40	–	[38]
$\mu_{C,i}$ ( $i=1,2$ )	$1.0 \cdot 10^{-3}$	1/h	[39]
$\mu_i'$ ( $i=1,2$ )	2.646	ng/(mm <sup>2</sup> h)	[29]
$k_{ECM1,i}$ ( $i=1$ )	$0.017 \cdot 10^3$	dw% mm <sup>6</sup> /(ng mmol h)	[29]
$k_{ECM2,i}$ ( $i=1,2$ )	$0.015 \cdot 10^3$	dw% mm <sup>6</sup> /(ng mmol h)	[29]
$k_{ECM1,i}$ ( $i=2$ )	$12.7 \cdot 10^3$	dw% mm <sup>6</sup> /(ng mmol h)	[30]
$a_{ij}$ ( $i=1; j=1$ )	$0.30 \cdot 10^{-3}$	1/h	[30]
$b_{ij}$ ( $i=1; j=1$ )	$0.07 \cdot 10^{-3}$	ng/mm <sup>3</sup>	[30]
$\chi_{ij}$ ( $i=1; j=1$ )	$0.68 \cdot 10^{-3}$	ng of GF/ng of cells	[30]

who investigated the *LIF-induced* differentiation of multipotent neural stem cells of murine central nervous system into astrocytes enhanced by *Activin A*. Murine stem cells were seeded onto poly-L-lysine, fibronectin, laminin-coated glass coverslips and were cultivated with 10 ng/ml of *LIF*. The effect of *activin A* on the stem cell differentiation of *MEB5* line into astrocytes was investigated by adding 1 or 10 or 100 ng/ml of this growth factor. Model parameters used in simulation run, whose values are reported in table 5, are taken from the literature related to either the original work from which the experimental data have been generated or to specific sources where the corresponding values are available. It should be noted that parame-

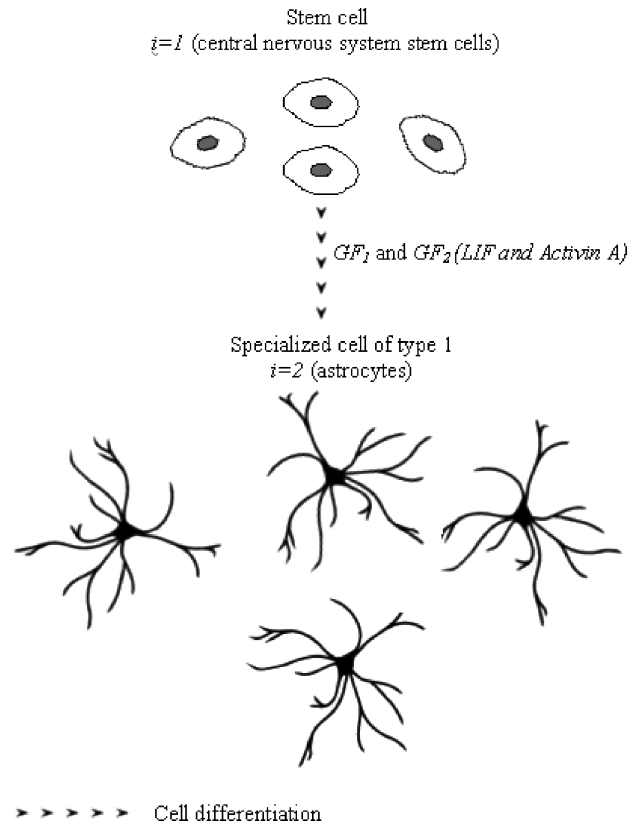


Fig. 7 – Schematic pathway for central nervous system stem cells differentiation into astrocytes stimulated by *LIF* and *Activin A*

Table 5 – Model parameters used in the simulation of the differentiation of murine central nervous system stem cells into astrocytes adding 10 ng/ml of *LIF* in the cultivation system.  $i=1$  for stem cells,  $i=2$  for astrocytes;  $j=1$  for *LIF*. Experimental data from Satoh et al.<sup>40</sup>

Parameter	Value	Unit	Reference
$n_i^0$ ( $i=1$ )	$2.0 \cdot 10^5$	cells	[40]
$n_i^0$ ( $i=2$ )	0	cells	[40]
$C_{GF_j}^0$ ( $j=1$ )	$10 \cdot 10^{-3}$	ng/mm <sup>3</sup>	[40]
$dc_i$ ( $i=1,2$ )	$1.14 \cdot 10^6$	ng/mm <sup>3</sup>	[33]
$C_{O_2}$	$0.124 \cdot 10^{-6}$	mmol/mm <sup>3</sup>	[36]
$C_m$	$0.006 \cdot 10^{-6}$	mmol/mm <sup>3</sup>	[36]
$\mu_{0,i}$ ( $i=1,2$ )	0.4	ng	[37]
$\sigma_i$ ( $i=1,2$ )	0.125	ng	[38]
$q_i$ ( $i=1,2$ )	40	–	[38]
$\mu_{C,i}$ ( $i=1,2$ )	$1.0 \cdot 10^{-3}$	1/h	[39]
$\mu_i'$ ( $i=1,2$ )	18.8	ng/(mm <sup>2</sup> h)	[31]
$\chi_{ij}$ ( $i=1; j=1$ )	$3.80 \cdot 10^{-4}$	ng of GF/ng of cells	[31]
$a_{ij}$ ( $i=1; j=1$ )	$1.05 \cdot 10^{-2}$	1/h	[31]
$b_{ij}$ ( $i=1; j=1$ )	$0.07 \cdot 10^{-3}$	ng/mm <sup>3</sup>	[31]



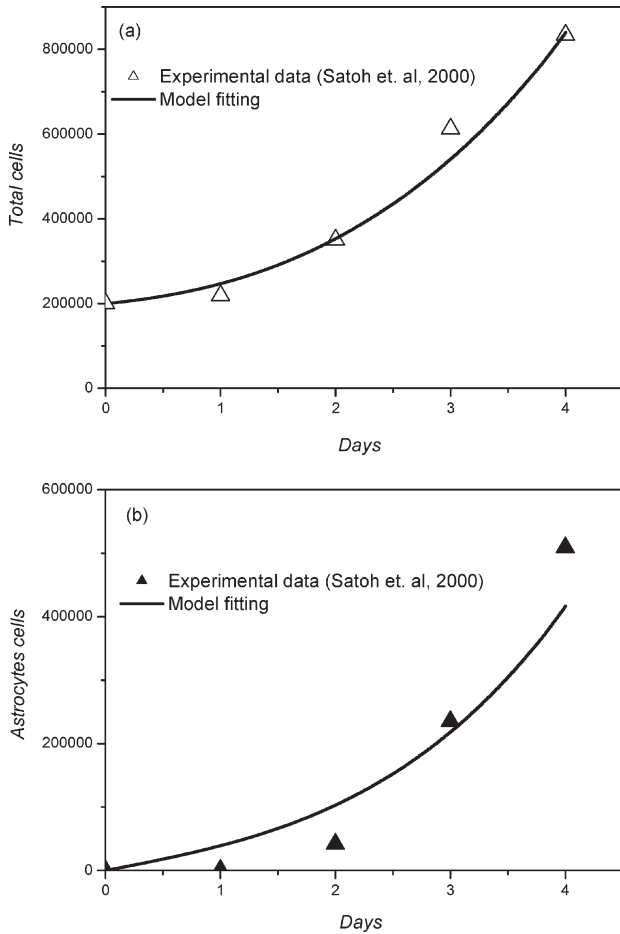


Fig. 8 – Comparison between model results and experimental data<sup>40</sup> in terms of total cells (a) and astrocytes number (b) as a function of cultivation time when 10 ng/ml of LIF are used during cell cultivation

ters  $q$ ,  $\mu_0$ ,  $\sigma$  and  $\mu'$  are the same for each type of cells since we do not have specific information for murine stem cells and astrocytes. Figs 8a and 8b show a good agreement between model results and experimental data in terms of total cells and astrocytes number, respectively, as a function of cultivation time when 10 ng/ml of LIF are used during the cell cultivation. It is worth noting that the unknown model parameters (i.e.,  $a_{11}$ ,  $\chi_{11}$  and  $\mu'_i$ ) are properly tuned to simulate the experimental data.

Next, we compare model results with experimental data obtained when cultivation was carried out by using 10 ng/ml of LIF with an addition of 100 ng/ml of Activin A. Model parameters used in this simulation run are reported in table 6. Also in this case parameters  $q_i$ ,  $\mu_{0i}$ ,  $\sigma_i$  and  $\mu'_i$  are the same for each type of cells ( $i=1$  and  $i=2$ ). As shown in Figs 9a and 9b, the agreement between model results and experimental data in terms of total cells and astrocytes number as a function of cultivation time, is satisfactory.

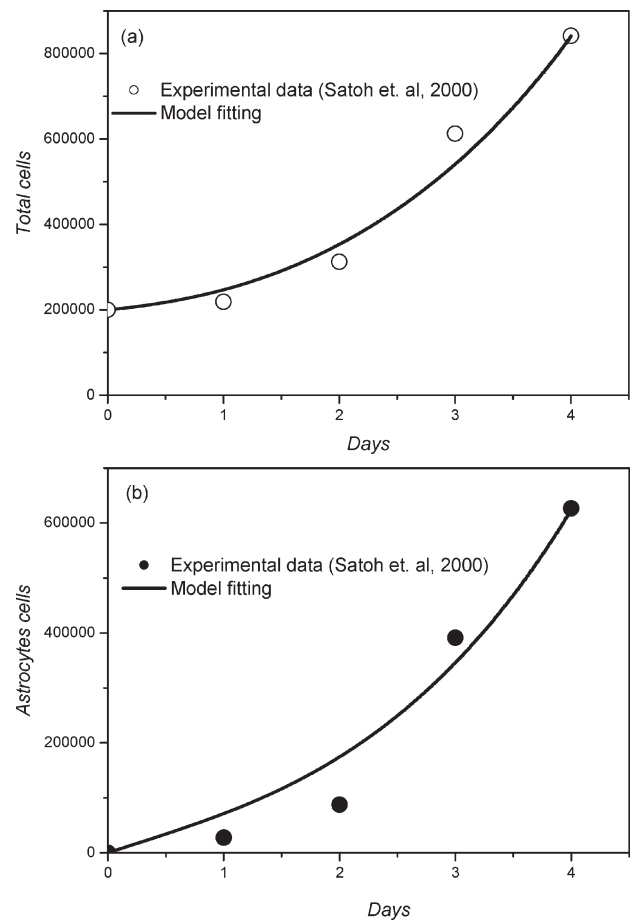


Fig. 9 – Comparison between model results and experimental data [40] in terms of total cells (a) and astrocytes number (b) as a function of cultivation time when 10 ng/ml of LIF and 100 ng/ml of Activin A are used during cell cultivation

It should be noted that, in this simulation, the only adjusted parameter is  $a_{12}$  (related to Activin A growth factor), while no change has been made in parameters  $a_{11}$ ,  $\chi_{11}$  (related to LIF) obtained from the previous calculation. Furthermore, it is assumed that  $b_{12} = b_{11}$  and  $\chi_{12} = \chi_{11}$ . To test the predictive model capability we then simulated the experimental data performed when different dosages of Activin A growth factor were used during the cell cultivation. By using the same parameters of table 6, i.e. without any fitting procedure, we compare model predictions and experimental data by Satoh et al.<sup>40</sup> in terms of astrocytes percentage as a function of added Activin A in the concentration range 0–100 ng/ml after 3 days of cell cultivation. The good agreement between model results and experimental data shown in Fig. 10 demonstrates the predictive capability of the model.

It is possible to observe that the augmentation of Activin A increases the differentiation of stem cells into astrocytes but this effect is not evident

Table 6 – Model parameters used in the simulation of the differentiation of murine central nervous system stem cells into astrocytes adding 10 ng/ml of LIF and 100 ng/ml of Activin A in the cultivation system.  $i=1$  for stem cells,  $i=2$  for astrocytes;  $j=1$  for LIF,  $j=2$  for Activin A. Experimental data from Satoh et al.<sup>40</sup>

Parameter	Value	Unit	Reference
$n_i^0$ ( $i=1$ )	$2.0 \cdot 10^5$	cells	[40]
$n_i^0$ ( $i=2$ )	0	cells	[40]
$C_{GF_j}^0$ ( $j=1$ )	$10 \cdot 10^{-3}$	ng/mm <sup>3</sup>	[40]
$C_{GF_j}^0$ ( $j=2$ )	$100 \cdot 10^{-3}$	ng/mm <sup>3</sup>	[40]
$dc_i$ ( $i=1,2$ )	$1.14 \cdot 10^6$	ng/mm <sup>3</sup>	[33]
$C_{O_2}$	$0.124 \cdot 10^{-6}$	mmol/mm <sup>3</sup>	[36]
$C_m$	$0.006 \cdot 10^{-6}$	mmol/mm <sup>3</sup>	[36]
$\mu_{0,i}$ ( $i=1,2$ )	0.4	ng	[37]
$\sigma_i$ ( $i=1,2$ )	0.125	ng	[38]
$q_i$ ( $i=1,2$ )	40	-	[38]
$\mu_{c,i}$ ( $i=1,2$ )	$1.0 \cdot 10^{-3}$	1/h	[39]
$\mu_i'$ ( $i=1,2$ )	18.8	ng/(mm <sup>2</sup> h)	[31]
$\chi_{ij}$ ( $i=1; j=1; j=2$ )	$3.80 \cdot 10^{-4}$	ng of GF/ng of cells	[31]
$a_{ij}$ ( $i=1; j=1$ )	$1.05 \cdot 10^{-2}$	1/h	[31]
$a_{ij}$ ( $i=1; j=2$ )	$0.39 \cdot 10^{-2}$	1/h	[31]
$b_{ij}$ ( $i=1; j=1; j=2$ )	$0.07 \cdot 10^{-3}$	ng/mm <sup>3</sup>	[31]

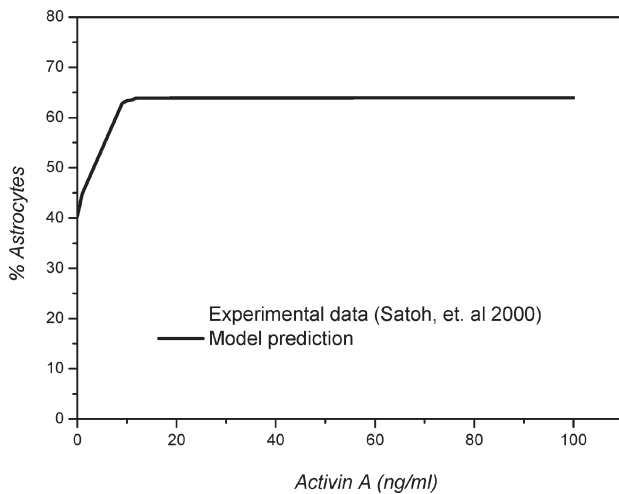


Fig. 10 – Comparison between model prediction and experimental data [40] in terms of astrocytes content (%) as a function of Activin A added during cell cultivation.

when the concentration of this growth factor is equal or greater to about 20 ng/ml. This behavior is well predicted by the model which therefore could be an useful tool to optimize the growth factor dosage during cell cultivation and differentiation.

## Concluding remarks

In the present work the capability of a novel mathematical model to simulate stem cells differentiation into specialized cells is demonstrated. The model, along the lines of our previous contributions [27–31], is based upon material balances for extra cellular matrix compounds, growth factors and nutrients as well as mass-structured population balance to simulate cell growth, differentiation and proliferation in vivo or during in vitro cultivation. The proposed model is written in a general form and may be used to simulate a generic cell differentiation pathway occurring during in vitro cultivation of connective and non-connective tissues.

Literature experimental data concerning the differentiation of stem cells into specialized ones are successfully compared with model results, thus demonstrating the validity of the proposed model, as well as its predictive capability.

The proposed mathematical model may be easily extended by accounting for the presence of drugs which may inhibit cell proliferation and/or differentiation. This can be done by introducing specific kinetic equations based upon typical enzyme-drug complex formation able to mimic the biologic behavior of proliferating cells in the presence of drugs. Therefore, this modeling approach appears particularly useful in predicting evolution, under pharmacologic treatment, of some iper-proliferative diseases such as tumors and restenosis.

## Notation

- $a$  – parameter appearing in equation (8) and (11), 1/h
- $b$  – parameter appearing in equation (8) and (11), ng/mm<sup>3</sup>
- $C_{ECM1}$  – concentration of GAG, dw%
- $C_{ECM2}$  – concentration of collagen, dw%
- $C_{GF}$  – concentration of growth factor, ng/mm<sup>3</sup>
- $C_{O_2}$  – concentration of O<sub>2</sub> at saturation condition, mmol/mm<sup>3</sup>
- $C^L$  – maximum collagen or GAG concentration, dw%
- $C_m$  – oxygen concentration at half-maximal consumption, mmol/mm<sup>3</sup>
- $d$  – mass density, ng/mm<sup>3</sup>
- $f(m)$  – division probability density function
- $k_{ECM1}$  – rate constant for GAG synthesis, dw% mm<sup>6</sup>/(ng mmol h)
- $k_{ECM2}$  – rate constant for collagen synthesis, dw% mm<sup>6</sup>/(ng mmol h)
- $k_{GF}^B$  – rate constant for *in vivo* GF synthesis, ng of GF/(ng of cells h)
- $m$  – single cell mass, ng
- $N_C$  – number of cell type
- $N_{GF}$  – number of growth factors

- $N_m$  – number of grid points for the mass domain  
 $p$  – partitioning function  
 $q$  – coefficient appearing in symmetric beta function  
 $t$  – cultivation time, h

### Greek letters

- $\beta(q, q)$  – symmetric beta function  
 $\Gamma^F$  – division rate function, 1/h  
 $\Gamma^T$  – differentiation rate function, 1/h  
 $\mu_0$  – average mass of dividing cells, ng  
 $\mu'$  – maximum rate of cell growth, ng/(mm<sup>2</sup> h)  
 $\mu_c$  – catabolic rate, 1/h  
 $\nu$  – time rate of change of cell mass  $m$ , ng/h  
 $\rho$  – cell number per unit volume, cells/mm<sup>3</sup>  
 $\rho^0$  – initial cell number per unit volume, cells/mm<sup>3</sup> or cells/pellets  
 $\sigma$  – standard deviation of the Gaussian distribution, ng  
 $\chi$  – yield appearing in equation (11), ng of GF/ng of cells  
 $\psi$  – cell distribution function, cells/(ng mm<sup>3</sup>)

### Superscripts

- 0 – initial conditions  
 ' – mother cell

### Subscripts

- $c$  – cells  
 $E_{CM1}$  – component of ECM, glycosaminoglycan (GAG)  
 $E_{CM2}$  – component of ECM, collagen  
 $GF$  – growth factor  
 $i$  –  $i$ -th cell type  
 $j$  –  $j$ -th growth factor  
 $k$  –  $k$ -th cell type  
 $O_2$  – oxygen  
 $w$  – water

### References

- Baksh, D., Song, L., Tuan, R. S., Adult mesenchymal stem cells: characterization, differentiation, and application in cell and gene therapy. *Journal of Cellular Molecular Medicine* **8** (2004) 301.
- Khademhosseini, A., Zandstra, P. W., Engineering the *in vitro* cellular microenvironment for the control and manipulation of adult stem cell responses. In: *Turksen, K.* (Ed). *Adult Stem Cells*. The Humana Press Inc., Totowa, NJ (2004) 289.
- Kuo, C. K., Tuan, R. S., Tissue engineering with mesenchymal stem cells. *IEEE Engineering in Medicine and Biology Magazine* **22** (2003) 51.
- Caplan, A. I., Bruder, S. P., Mesenchymal stem cells: building blocks for molecular medicine in the 21<sup>st</sup> century. *TRENDS in Molecular Medicine* **7** (2001) 259.
- Barry, F., Boynton, R. E., Liu, B., Murphy, J. M., Chondrogenic differentiation of mesenchymal stem cells from bone marrow: differentiation-dependent gene expression of matrix component. *Experimental Cell Research* **268** (2001) 189.
- Alhadlaq, A., Mao, J. J., Mesenchymal stem cells: Isolation and Therapeutics. *Stem Cells and Development* **13** (2004) 436.
- Taqvi, S., Roy, K., Influence of scaffold physical properties and stromal cell coculture on hematopoietic differentiation of mouse embryonic stem cells. *Biomaterials* **27** (2006) 6024.
- Willerth, S. M., Arendas, K. J., Gottlieb, D. I., Sakiyama-Elbert, S. E., Optimization of fibrin scaffolds for differentiation of murine embryonic stem cells into neural lineage cells. *Biomaterials* **27** (2006) 5990.
- Yamaguchi, A. (1995) Regulation of differentiation pathway of skeletal mesenchymal cells in cell lines by transforming growth factor- $\beta$  superfamily. *Seminars in Cell Biology*, **6**, 165.
- Johnstone, B., Hering, T. M., Caplan, A. I., Goldberg, V. M., Yoo, J. U., In vitro chondrogenesis of bone marrow-derived mesenchymal progenitor cells. *Experimental Cell Research* **238** (1998) 265.
- Worster, A. A., Brower-Toland, B. D., Fortier, L. A., Bent, S. J., Williams, J., Nixon, A. J., Chondrocytic differentiation of mesenchymal stem cells sequentially exposed to transforming growth factor- $\beta$ 1 in monolayer and insuline-like growth factor-I in a three-dimensional matrix. *Journal of Orthopaedic Research* **19** (2001) 738.
- Bai, X., Xiao, Z., Pan, Y., Hu, J., Pohl, J., Wen, J., Li, L., Cartilage-derived morphogenetic protein-1 promotes the differentiation of mesenchymal stem cells into chondrocytes. *Biochemical and Biophysical Research Communications* **325** (2004) 453.
- Bosnakovski, D., Mizuno, M., Kim, G., Ishiguro, T., Okumura, M., Iwanaga, T., Kadosawa, T., Fujinaga, T., *Experimental Hematology* **32** (2004) 502.
- Tsuchiya, K., Chen, G., Ushida, T., Matsuno, T., Tateishi, T., *Material Science Engineering C* **24** (2004) 391.
- Chen, C. W., Tsai, Y. H., Deng, W. P., Shih, S. N., Fang, C. L., Burch, J. G., Chen, W. H., Lai, W. F., Type I and II collagen regulation of chondrogenic differentiation by mesenchymal progenitor cells. *Journal of Orthopaedic Research* **23** (2005) 446.
- Li, W. J., Tuli, R., Okafor, C., Derfoul, A., Danielson, K. G., Hall, D. J., Tua, R. S., *Biomaterials* **26** (2005) 599.
- Mauch, R. L., Yuan, X., Tsuan, R. S., Chondrogenic differentiation and functional maturation of bovine mesenchymal stem cells in long-term agarose culture. *Osteoarthritis and Cartilage* **14** (2006) 179.
- Till, J. E., McCulloch, E. A., Siminovitch, L. A stochastic model of stem cell proliferation, based on growth of spleen colony-forming cells. *Proc. Natl Acad. Sci. USA*. **51** (1964) 29.
- Nielsen, L. K., Papoutsakis, L. K., Miller, W. M., Modeling ex-vivo hematopoiesis using chemical engineering metaphors. *Chemical Engineering Science* **53** (1998) 1913.
- Bailon-Plaza, A., van der Meulen, M. C. H., A mathematical framework to study the effects of growth factor influences on fracture healing. *Journal of Theoretical Biology* **212** (2001) 191.
- Hentschel, H. G. E., Glimm, T., Glazier, J. A., Newman, S. A., Dynamical mechanisms for skeletal pattern formation in the vertebrate limb. *Proc. R. Soc. Lond. B.* **271** (2004) 1713.

22. Mehr, R., Globerson, A., Perelson, A. S., Modeling positive and negative selection of differentiation processes in the thymus. *Journal of theoretical biology* **175** (1995) 103.
23. Yu, A., Mayer-Proschel, M., Noble, M., A stochastic model of brain cell differentiation in tissue culture. *Journal of Mathematical Biology* **37** (1998) 49.
24. Zorin, A., Mayer-Proschel, M., Noble, M., Yakovlev, A. Y., Estimation problem associated with stochastic modeling of proliferation and differentiation of O2-A progenitor cells *in vitro*. *Mathematical Biosciences* **167** (2000) 109.
25. Cinquin, O., Demongeot, J., High-dimensional switches and the modelling of cellular differentiation. *Journal of Theoretical Biology* **233** (2005) 391.
26. Roeder, I., Glauche, I., Towards an understanding of lineage specification in hematopoietic stem cells: a mathematical model for the interaction of transcription factors GATA-1 and PU-1. *Journal of Mathematical Biology* **241** (2006) 852.
27. Pisu, M., Lai, N., Cincotti, A., Delogu, F., Cao, G., A simulation model for the growth of tissue engineered cartilage on polymeric scaffolds. *International Journal of Chemical Reactor Engineering*. Available at <http://www.bepress.com/ijcre/vol1/A38>, 2003.
28. Pisu, M., Lai, N., Cincotti, A., Concas, A., Cao, G., Model of engineered cartilage growth in rotating bioreactors. *Chemical Engineering Science* **59** (2004) 5035.
29. Pisu, M., Concas, A., Lai, N., Cao, G., A novel simulation model for engineered cartilage growth in static systems. *Tissue Engineering* **12** (2006) 2311.
30. Pisu, M., Concas, A., Cao, G., A novel simulation model for stem cells differentiation. *Journal of Biotechnology* **130** (2007) 171.
31. Pisu, M., Concas, A., Fadda, S., Cincotti, A., Cao, G., A simulation model for stem cells differentiation into specialized cells of non-connective tissues. *Journal of Computational Biology and Chemistry* **32** (2008) 338.
32. Wilson, C. G., Bonassar, L. J., Kohles, S. S., Modeling the dynamic composition of engineered cartilage. *Archives of Biochemistry and Biophysics* **408** (2002) 246.
33. Jakob, M., Demarteau, O., Schafer, D., Stumm, M., Heberer, M., Martin, I., Enzymatic digestion of adult human articular cartilage yields a small fraction of the total available cells. *Connective Tissue Research* **44** (2003) 173.
34. Basser, P. J., Schneiderman, R., Bank, R. A., Watchel, E., Maroudas, A., Mechanical properties of the collagen network in human articular cartilage as measured by osmotic stress technique. *Archives of Biochemistry and Biophysics* **351** (1998) 207.
35. Perry, R. H., Green, D. W., eds. *Perry's Chemical Engineers' Handbook*, Seventh Edition. New York: McGraw Hill; 1997.
36. Obradovic, B., Meldon, J. H., Freed, L. E., Vunjak-Novakovic, G., Glycosaminoglycan deposition in engineered cartilage: experiments and mathematical model. *AIChE Journal* **46** (2000) 1860.
37. Kupsco, J., Master's Thesis. University of Richmond 2001. Available at [http://oncampus.richmond.edu/~gradice/Kupsco\\_thesis.html](http://oncampus.richmond.edu/~gradice/Kupsco_thesis.html).
38. Mantzaris, N. V., Liou, J. J., Daoutidis, P., Srienc, F., Numerical solution of a mass structured cell population balance in an environment of changing substrate concentration. *Journal of Biotechnology* **71** (1999) 157.
39. Munteanu, S. E., Ilic, M. Z., Handley, C. J., Highly sulfated glycosaminoglycans inhibit aggrecanase degradation of aggrecan by bovine articular cartilage explant culture. *Matrix Biology* **21** (2002) 429.
40. Satoh, M., Sugino, H., Yoshida, T., Activin promotes astrocytic differentiation of a multipotent neural stem cell line and an astrocyte progenitor cell line from murine central nervous system. *Neuroscience Letters* **284** (2000) 143.